

PROCEEDINGS OF SPIE

SPIEDigitalLibrary.org/conference-proceedings-of-spie

Image-based temporal alignment of echocardiographic sequences

Adriyana Danudibroto, Jørn Bersvendsen, Oana Mirea, Olivier Gerard, Jan D'hooge, et al.

Adriyana Danudibroto, Jørn Bersvendsen, Oana Mirea, Olivier Gerard, Jan D'hooge, Eigil Samset, "Image-based temporal alignment of echocardiographic sequences," Proc. SPIE 9790, Medical Imaging 2016: Ultrasonic Imaging and Tomography, 97901G (1 April 2016); doi: 10.1117/12.2216192

SPIE.

Event: SPIE Medical Imaging, 2016, San Diego, California, United States

Image-based temporal alignment of echocardiographic sequences

Adriyana Danudibroto^{a,b}, Jørn Bersvendsen^{a,c}, Oana Mirea^b, Olivier Gerard^a, Jan D'hooge^b,
and Eigil Samset^{a,c}

^aGE Vingmed Ultrasound, Oslo, Norway

^bDept. of Cardiovascular Imaging and Dynamics, KU Leuven, Belgium

^cUniversity of Oslo, Norway

ABSTRACT

Temporal alignment of echocardiographic sequences enables fair comparisons of multiple cardiac sequences by showing corresponding frames at given time points in the cardiac cycle. It is also essential for spatial registration of echo volumes where several acquisitions are combined for enhancement of image quality or forming larger field of view. In this study, three different image-based temporal alignment methods were investigated. First, a method based on dynamic time warping (DTW). Second, a spline-based method that optimized the similarity between temporal characteristic curves of the cardiac cycle using 1D cubic B-spline interpolation. Third, a method based on the spline-based method with piecewise modification. These methods were tested on in-vivo data sets of 19 echo sequences. For each sequence, the mitral valve opening (MVO) time was manually annotated. The results showed that the average MVO timing error for all methods are well under the time resolution of the sequences.

Keywords: 3D echocardiography, temporal alignment, temporal registration, Dynamic Time Warping, 1D cubic B-spline

1. INTRODUCTION

3D echocardiography is used in daily clinical settings for assessing the morphology and function of the heart. In comparison to other modalities, it has relatively low cost, high frame rate and no ionizing radiation. However, tuning the acquisition to a fair spatiotemporal resolution oftentimes results in a field of view that is too narrow for capturing the whole structure of interest. To address this issue, solutions based on combining several acquisitions to form one wide field of view recording have been proposed.¹⁻⁴ The first part of these solutions consisted of a registration between the sequences. However, echo sequences contain recordings of a dynamic organ which requires registration in both the space and time dimension.

Image registration solutions for 3D echo in the literature rarely discussed temporal alignment.^{1,2,4} These solutions performed registration only on the end-diastolic (ED) frame. On the other hand, Mulder et al. addressed this issue by manually identifying the ED and end-systolic (ES) frames,³ which is tedious when done on large data sets and also prone to inter-observer variability. Henceforth, an image-based temporal alignment offers more automated and consistent results.

Previous work has been done on image-based temporal alignment for cardiac MRI sequences⁵ and cardiac MRI to 3D echo sequences.^{6,7} These methods used a temporal characteristic curve that is derived solely from the recording, without using externally measured data such as ECG. The temporal characteristic curve is based on the normalized cross correlation (NCC) curve measured over time. It has been shown that this curve is able to succinctly describe the cardiac cycle characteristics.⁷ A comparison of three methods is presented in this study; these are: 1) dynamic time warping (DTW) method by Perissinotto et al.,⁷ 2) a combined method of Perperidis et al.⁵ and Zhang et al.⁶ using 1D cubic B-spline interpolation on the temporal NCC curve and 3) a modified 1D cubic B-spline method which includes piecewise linear transform similar to the work of Shekhar et al.⁸ for distinction of systolic and diastolic phases alignment.

Corresponding author: A.Danudibroto

E-mail: adriyana.danudibroto@kuleuven.be

2. METHODS

Temporal alignment of two cardiac sequences aims to pair frames at corresponding time points in the cardiac cycle. The first step of the alignment is to compactly describe the temporal characteristic of each frame in the recordings which, in this study, was done using the temporal NCC curve. Then, the next step is to align corresponding frames by minimizing the differences between the temporal characteristic curves.

2.1 Temporal characteristic curve

The temporal NCC curve was chosen for its ability to represent the cardiac cycle events compactly, which has been demonstrated by the work of Perissinotto et al.⁷ and Zhang et al.⁶ Its shape closely matches the left ventricle volume curve and its minimum is associated with the ES event.⁷ The curve was computed as follows:

$$r(t) = \frac{\sum_x \sum_y \sum_z (f(x, y, z, t) - \bar{f}(t))(f(x, y, z, ED) - \bar{f}(ED))}{\sqrt{\sum_x \sum_y \sum_z (f(x, y, z, t) - \bar{f}(t))^2} \sqrt{\sum_x \sum_y \sum_z (f(x, y, z, ED) - \bar{f}(ED))^2}}, \quad (1)$$

where f is the 3D echo recording in assessment, \bar{f} is the average intensity of all the voxels in the 3D echo volume at a given time point and M_x, M_y, M_z are the volume dimension in x, y, z direction respectively. For speed, the sequence $f(x, y, z, t)$ was binarized using a threshold value of half of the intensity range prior to the $r(t)$ computation. The r curve was then normalized to the range of 0 to 1. An example of the temporal NCC curve for a reference and floating sequences can be seen in Figure 1 (left).

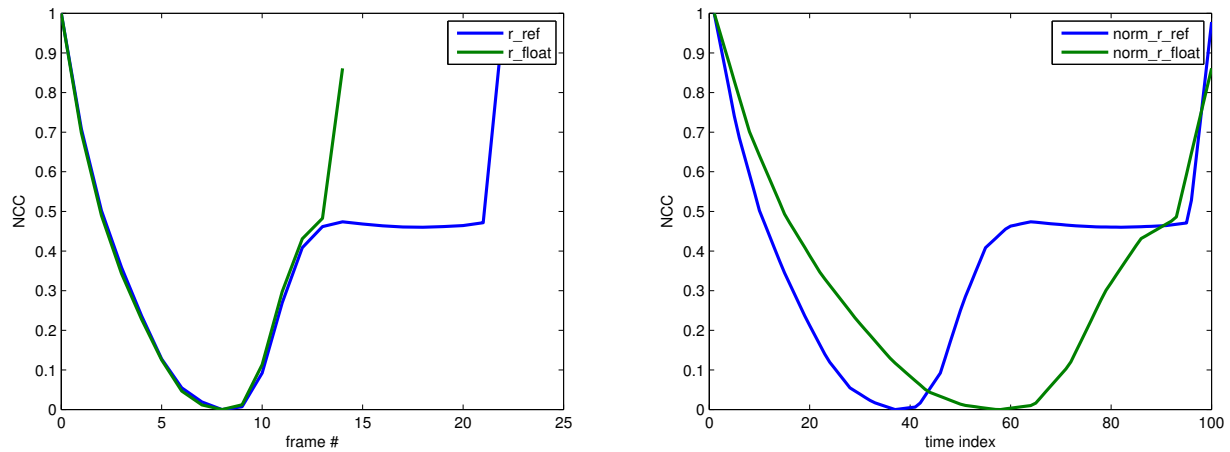


Figure 1. Temporal NCC curve of reference and floating sequence before (left) and after temporal normalization (right).

2.2 Dynamic time warping

The DTW method seeks for the path of least resistance to pair up the corresponding time points in temporal sequences. It warps one temporal NCC curve as closely as possible to another. In this implementation, first of all, the temporal resolution of the temporal NCC curve is increased by linearly interpolating the number of time samples to $N = 100$. An example of temporal normalization result is shown in Figure 1 (right). To find the optimal path for pairing the corresponding time points between the curves, a cost matrix was computed. The cost matrix consisted of squared differences between each element in the two curves and was computed as follows:

$$C(t_{ref}, t_{float}) = (r_{ref}(t_{ref}) - r_{float}(t_{float}))^2, \quad t_{ref}, t_{float} \in \{[1, N] \cap \mathbb{Z}^+\} \quad (2)$$

where r_{ref} and r_{float} are the temporal NCC curves of the reference and floating sequences respectively and t_{ref} and t_{float} are their respective time indices. Note that only integer time indices between 1 to N were considered. An example of a cost matrix between two sequences can be seen in Figure 2 (top left).

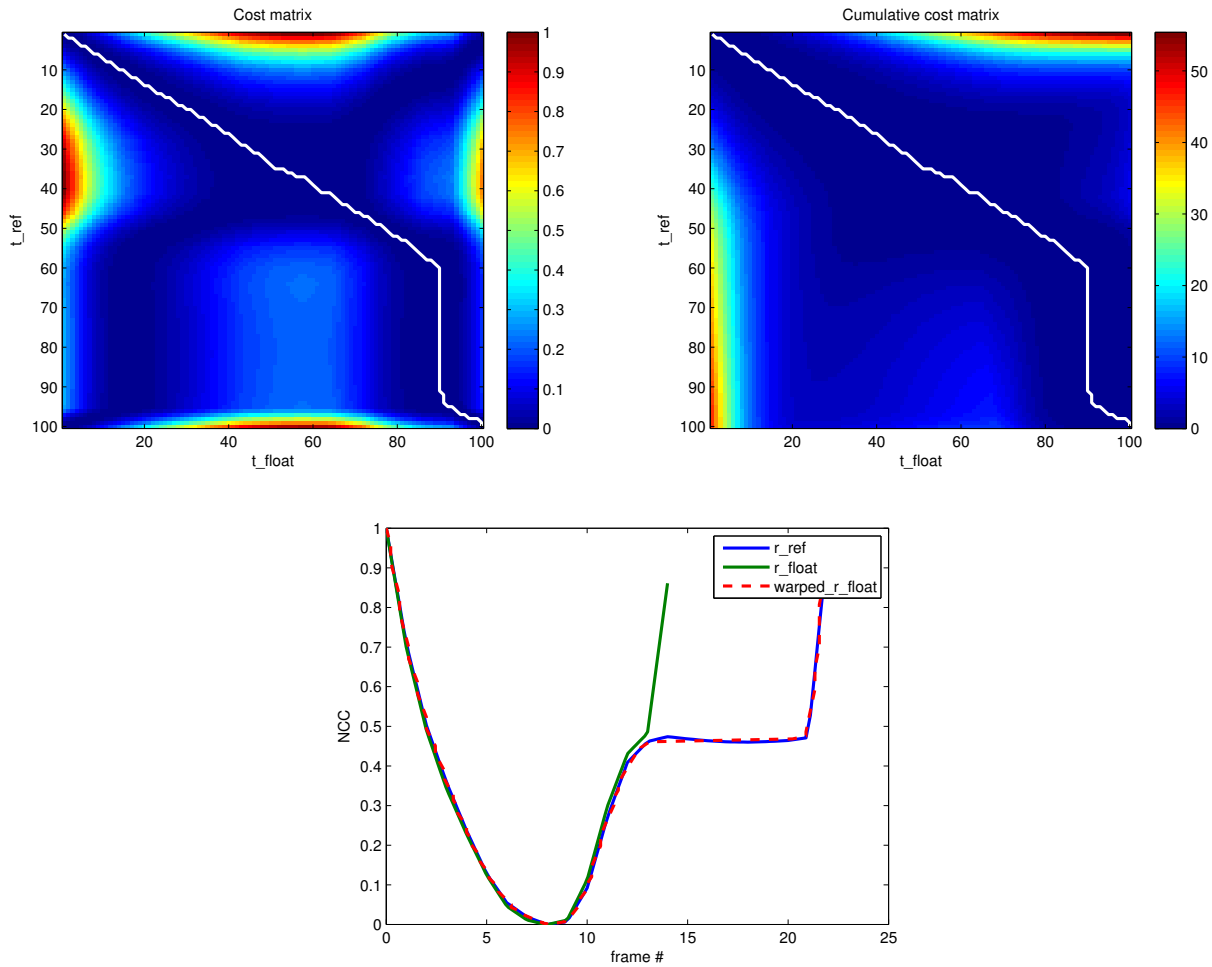


Figure 2. Cost matrix (top left) and cumulative cost matrix (top right) between reference and floating sequence and the optimal path shown in white. Temporal NCC curve of reference, floating and warped sequence using DTW method are also shown (bottom).

To find the optimal path starting from $(t_{ref}, t_{float}) = (1, 1)$ to $(t_{ref}, t_{float}) = (N, N)$, the cumulative cost matrix D was computed as follows:

$$\begin{aligned}
 \text{for } t_{ref} = 1, \quad D(1, t_{float}) &= \sum_{k=1}^{t_{float}} C(1, k) \\
 \text{for } t_{float} = 1, \quad D(t_{ref}, 1) &= \sum_{k=1}^{t_{ref}} C(k, 1) \\
 \text{for } t_{ref}, t_{float} \in (1, N], \quad D(t_{ref}, t_{float}) &= C(t_{ref}, t_{float}) + \\
 &\quad \min \{D(t_{ref} - 1, t_{float}), D(t_{ref}, t_{float} - 1), D(t_{ref} - 1, t_{float} - 1)\}.
 \end{aligned} \tag{3}$$

These conditions put a restriction on the step size of the path to $(1, 0)$, $(0, 1)$ and $(1, 1)$ which ensured that each frame in the sequences were visited. The optimal path was then found by finding the minimum per row or per

column of D . An example of a cumulative cost matrix and its optimal path can be seen in Figure 2 (top right). The resulting warped floating sequence according to the optimal path is shown in Figure 2 (bottom).

2.3 Spline-based alignment

Two spline-based methods were investigated in this study where one is a piecewise modification of the other. Both spline-based methods consist of two parts: a global transform and a local transform. The global transform is responsible for aligning the difference in sequence length through linear scaling and the local transform aims to minimize the disparity between the shapes of the NCC curves. The first spline-based method was modeled as follows:

$$T(t) = T_{global}(t) + T_{local}(t). \quad (4)$$

The piecewise modification of the spline based method was done to handle the alignment of systolic and diastolic phases independently. The separation between the systolic and diastolic phases was found by detecting the minimum of the temporal NCC curve which corresponds to the ES time point. The method was modeled as follows:

$$\begin{aligned} T(t) = & T_{global_{systolic}}(t) + T_{local_{systolic}}(t) \quad \text{for } t \in [0, ES] \\ & T_{global_{diastolic}}(t) + T_{local_{diastolic}}(t) \quad \text{for } t \in (ES, end]. \end{aligned} \quad (5)$$

For both spline-based methods, the local transform was modeled as a 1D cubic B-spline as follows:

$$T_{local}(t) = \sum_{i=1}^{N_t} b_i \left(\frac{t}{T_s} \right) \tau_i, \quad (6)$$

where T_s is the length of the temporal NCC curve, b_i is a B-spline basis function, N_t is the number of spline knots and τ_i is the control time displacement which was computed by:

$$\arg \min_{\tau} |r_{ref}(t) - r_{float}(T(t))|^2. \quad (7)$$

The optimization was performed numerically by sequential quadratic programming and the transform T was restricted to be monotonically increasing to maintain the frame order. An example of the NCC curves for a reference and floating sequence pair, as well as the transformed curve using the spline-based and piecewise spline-based methods are shown in Figure 3 (left). The transform functions computed by spline-based and piecewise spline-based methods that were used to warp the floating sequence are also shown in Figure 3 (right).

2.4 Validation

The validation was done on in-vivo data sets of 19 3D echo recordings, acquired from 7 healthy subjects using a GE Vivid E9 system. All recordings contained an apical view with slightly varying view points, acquired using multibeam acquisition over 4 heart cycles. For reference, the time points of the mitral valve opening (MVO) were annotated manually in all recordings. The accuracy assessment was done by comparing the MVO timing between the reference sequence and the warped/transformed floating sequence.

As a benchmark against the three investigated methods, the global linear transform as the most straightforward method of aligning the sequences was also assessed. To assess the significance of the differences between the results, paired t-test analyses for two-tailed distributions with Bonferroni correction for multiple statistical tests were done.

In addition, the root mean square error (RMSE) was also computed between the reference and the warped floating NCC curves to indicate how well the warped curves followed the shape of reference curves. Moreover, to assess the correlation between the RMSE and MVO timing error, the R^2 Pearson's correlation coefficient was computed.

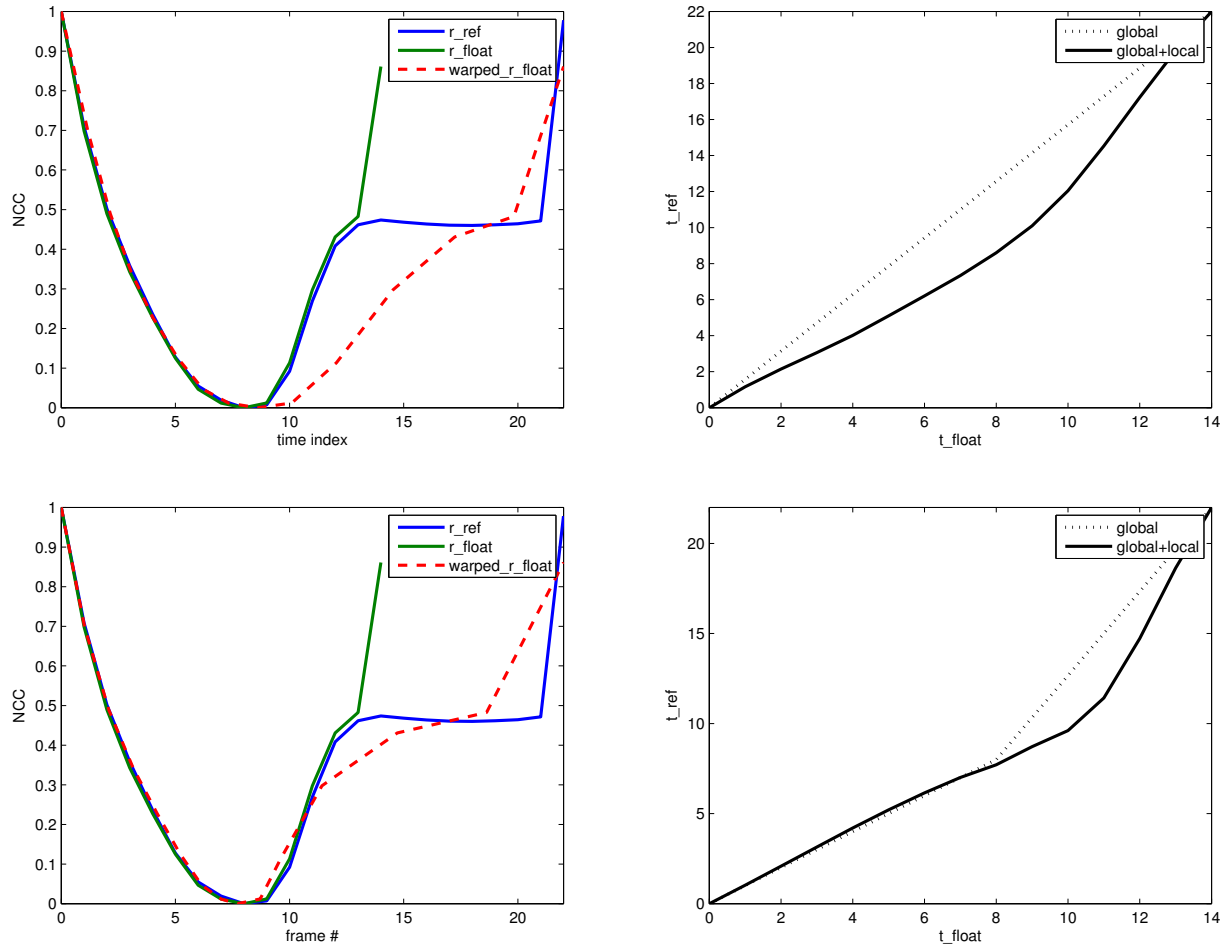


Figure 3. Temporal NCC curve of reference, floating and warped floating sequence (left column) and the transformation applied to the warped floating sequence (right column). Top row shows the result from the spline-based method, bottom row shows result from the piecewise spline-based method.

3. RESULTS

The investigated methods were implemented in MATLAB and experiments were run on an Intel Core i7-3740QM CPU at 2.7 GHz. A video showing an example reference and floating sequences as well as the resulting registered sequences with linear, DTW, spline-based and piecewise spline-based methods can be seen in Video 4. The sequences were spatially registered with the method proposed in our previous work.⁴

Two sequence pairs were removed from the analysis due to image quality reason. The MVO timing errors, RMSE and average computation times for all methods are shown in table 1. The computation times were calculated on the alignment of volume sequences with dimension 172x171x159 with an isometric voxel size of 1 mm.

For a reference, the average inter-frame time of all recordings was 47 ± 4 ms. All the investigated methods produced MVO timing error that are well under that figure. In terms of computation time, all methods performed on the same order of magnitude.

The paired t-test with multiple tests correction performed on the MVO timing error and RMSE from all methods against linear method resulted in $p < 0.05$. Moreover, in terms of RMSE, the DTW also achieved

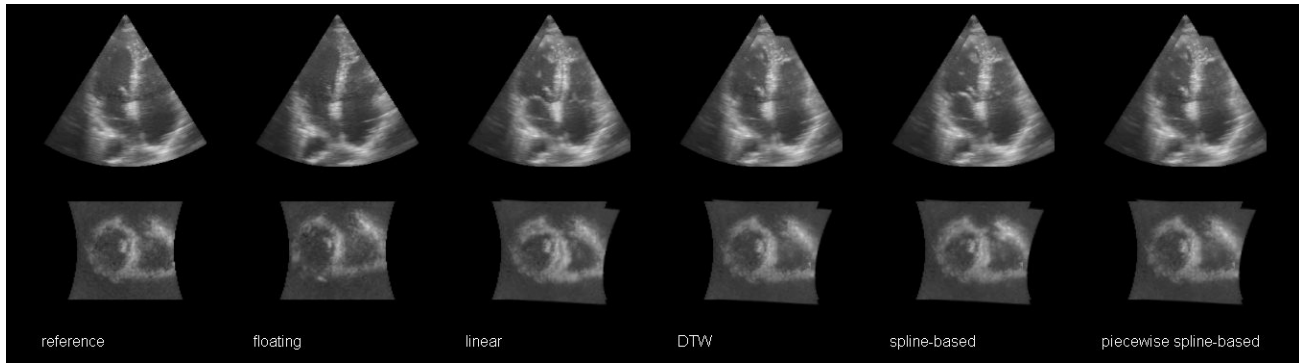


Figure 4. Video screen shot showing the results of temporal registration using all experimented methods and the reference and floating sequences <http://dx.doi.org/10.1117/12.2216192>.

significantly lower value in comparison to all the other methods ($p < 0.05$). The R^2 value between all MVO timing errors and RMSE is 0.73.

Table 1. Summary of results: mitral valve opening (MVO) timing error (ms), root mean squared error (RMSE) between the reference and warped floating sequences and computation time (ms).¹denotes $p < 0.05$ against linear method, ²denotes $p < 0.05$ against DTW method.

Method	Linear	DTW	Spline-based	Piecewise spline-based
MVO error (ms)	53±37	16±10 ¹	13±10 ¹	16±11 ¹
RMSE (*10 ⁻³)	80±40 ²	10±6 ¹	34±17 ^{1,2}	35±17 ^{1,2}
Computation time (ms)	-	838±19	831±23	840±24

4. DISCUSSION

The focus of this study was to compare different methods of temporal alignment for 3D echo sequences. Temporal alignment is required in the context of registration of multiple echo sequences because the heart is a dynamic organ. Temporal alignment helps to provide the correspondences between the same time points in the cardiac cycles that were recorded in the 3D echo sequences. Thus, the volumes can be compared fairly at corresponding time points. The example in Video 4 shows how the same spatial registration result is presented differently with different temporal alignment method.

Image-based methods that were investigated in this study relied heavily on the image quality. In relation to this issue, two outliers were removed before the data analysis due to image quality reason.

The results summary in table 1 shows that all investigated methods produced much smaller MVO timing error than the benchmark linear method ($p < 0.05$). The MVO timing error of the investigated methods are also well under the average temporal resolution of the sequences. The lowest MVO timing error was achieved by the spline-based method, however no statistical significance was observed against DTW and piecewise spline-based method.

It can also be seen that the DTW method resulted in the lowest RMSE among all other methods ($p < 0.05$) which indicates that it warped the floating NCC curves the closest to the reference curves. Moreover, the R^2 value between all MVO timing errors and RMSE which is 0.73 indicates that there is a positive correlation between them. Thus, the results showed that the DTW method performed the best.

However, it is still important to match the salient points in the temporal NCC curves, for example the minimum point that indicates the ES frame. This is demonstrated by the spline and piecewise spline-based

methods. In Figure 3 (top left), it can be seen that due to the relatively large discrepancy between the length of reference and floating sequences, the ES frame has gotten largely shifted by the global transform of the spline-based method. Thus, the local transform reached a local minimum before shifting the ES frame back to match the reference. On the other hand, the piecewise spline-based method took this into account by splitting the global and local transforms for systolic and diastolic phases, resulting in the exact match of the ES frame as seen in Figure 3 (bottom left).

5. CONCLUSION

Three image-based temporal alignment methods for 3D echo sequences were investigated and compared in this study. The three methods matched the corresponding events in the cardiac cycle through the temporal NCC curve which is a compact representation of the temporal characteristic of the 3D echo sequence.

The first implemented method was the DTW method which was able to warp the floating temporal NCC curve very closely to the reference temporal NCC curve. The second method was a spline-based method whose computed transform consisted of two parts: a global and local transform. The third method was the piecewise spline-based method which was a piecewise modification of the previously mentioned method.

The methods were tested on in-vivo data sets of 19 3D echo sequences with two sequence pairs removed before the data analysis due to image quality reason. To assess the temporal accuracy of the methods, the MVO event was manually annotated on each sequence. The results showed that DTW is the method that match the shape of the temporal NCC curve closest to the reference, while no statistical significant difference was observed in the accuracy of the three methods.

ACKNOWLEDGMENTS

This work is supported by Marie Curie Initial Training Network (USART-project, grant ID: PITN-GA-2012-317132).

REFERENCES

- [1] Grau, V., Becher, H., and Noble, J. A., "Phase-based registration of multi-view real-time three-dimensional echocardiographic sequences," in [*MICCAI 2006*], Larsen, R., Nielsen, M., and Sparring, J., eds., *LNCS* **4190**, 612–619, Springer Berlin Heidelberg (2006).
- [2] Rajpoot, K., Grau, V., Noble, J. A., Szmigielski, C., and Becher, H., "Multiview fusion 3-D echocardiography: Improving the information and quality of real-time 3-D echocardiography," *UMB* **37**(7), 1056–1072 (2011).
- [3] Mulder, H. W., van Stralen, M., van der Zwaan, H. B., Leung, K. Y. E., Bosch, J. G., and Pluim, J. P. W., "Multiframe registration of real-time three-dimensional echocardiography time series," *J. Med. Imag.* **1**(1), 014004 (2014).
- [4] Danudibroto, A., Gerard, O., Alessandrini, M., Mirea, O., Dhooge, J., and Samset, E., "3D Farneback optic flow for extended field of view of echocardiography," in [*Functional Imaging and Modeling of the Heart*], van Assen, H., Bovendeerd, P., and Delhaas, T., eds., *Lecture Notes in Computer Science* **9126**, 129–136, Springer International Publishing (2015).
- [5] Perperidis, D., Mohiaddin, R. H., and Rueckert, D., "Spatio-temporal free-form registration of cardiac MR image sequences," *Medical image analysis* **9**(5), 441–456 (2005).
- [6] Zhang, W., Noble, J., and Brady, J., "Spatio-temporal registration of real time 3D ultrasound to cardiovascular MR sequences," in [*MICCAI 2007*], Ayache, N., Ourselin, S., and Maeder, A., eds., *LNCS* **4791**, 343–350, Springer Berlin Heidelberg (2007).
- [7] Perissinotto, A., Queirós, S., Morais, P., Baptista, M. J., Monaghan, M., Rodrigues, N. F., D'hooge, J., Vilaa, J. L., and Barbosa, D., "Robust temporal alignment of multimodal cardiac sequences," *Proc. SPIE* **9413**, 94131K–94131K–9 (2015).
- [8] Shekhar, R., Zagrodsky, V., Garcia, M. J., and Thomas, J. D., "Registration of real-time 3-d ultrasound images of the heart for novel 3-d stress echocardiography," *Medical Imaging, IEEE Trans. on* **23**(9), 1141–1149 (2004).